

Vacuum Stability Constraints and LHC Searches for a Model with a Universal Extra Dimension

Anindya Datta^{a,1} and *Sreerup Raychaudhuri*^{b,2}

^a Department of Physics, University of Calcutta,
92 Acharya Prafulla Chandra Road, Kolkata 700 009, India

^b Department of Theoretical Physics, Tata Institute of Fundamental Research,
1 Homi Bhabha Road, Mumbai 400005, India.

Abstract

If the new boson is lying in the narrow mass range between 122 - 127 GeV is confirmed to be a Higgs boson, then stability of the electroweak vacuum in a minimal model with a universal extra dimension (mUED) will require a much lower cutoff for the theory than has been envisaged earlier. We show that this low cutoff would lead to important changes in much of the mUED phenomenology studied till now. In particular, prospects for LHC searches for $n = 1$ states are rather limited, while resonant $n = 2$ states may go completely undetected. Prospects for detection at the ILC and CLIC are less affected.

Pacs Nos: 14.80.Ec, 14.80.Rt, 13.85.Qk

December 17, 2018

¹ adphys@caluniv.ac.in

² sreerup@theory.tifr.res.in

The Higgs sector has long been regarded as an Achilles heel for the Standard Model (SM), inasmuch as it calls for the induction of elementary scalar fields, for which there was not a shred of experimental evidence at the time when the SM was developed. Moreover, as soon as we attempt to embed the SM in a higher gauge symmetry, the mass of such an elementary scalar becomes unstable, and new physics has to be invoked to restore the model to consistency. Despite these obvious drawbacks, the simplicity of the Higgs model for electroweak symmetry-breaking has been attractive enough for it to be taken with all seriousness through several decades of searching for the Higgs boson. Now, at long last, it seems that a neutral Higgs boson of mass around 125 GeV has been discovered at the LHC [1]. Precise knowledge of the Higgs boson mass means that the last unknown parameter in the SM is now known, and since each particle mass in the SM is related to a coupling constant, this also means that all the interactions in the SM are fully known. More specifically, if $M_H \approx 125$ GeV, then the Higgs boson self-coupling λ is given, at the electroweak symmetry-breaking scale, by $\lambda = M_H^2/2v^2 \approx 0.129$.

Assuming that the discovered boson is a Higgs boson, as predicted in the SM and most of its extensions, the experimental data tell us that its mass must lie in the range 122 – 127 GeV [1, 2]. As it happens, this is a range where the Higgs boson leads a somewhat precarious existence, for as we increase the energy scale Q above the electroweak scale, there is a tendency for the running coupling $\lambda(Q)$ to be driven to smaller and smaller values, eventually becoming negative. If this happens, the scalar potential becomes unbounded from below, or, in the usual jargon, the electroweak vacuum becomes unstable. In the SM, however, this could happen at an energy scale in the ballpark of 10^{11} GeV [3] — which is well above the energy scale at which any present or foreseeable terrestrial experiment can be done. Presumably, some new physics will appear at a high scale before this point of instability is reached, and the vacuum of the new theory will be stable — obviously this would not be directly verifiable by experiment, but we can take the corresponding scale as the cutoff when calculating quantum corrections in the SM framework.

Since the scale where the new physics must appear is far below the Planck scale, a Higgs boson discovery in the range 122 – 127 GeV could indicate the existence of new physics beyond the SM. However, no definitive statement can be made in the frame work of the SM unless we have a more precise determination of the top quark pole mass [4]. More interestingly, the presence of new particles and interactions at or around the electroweak scale in models which go beyond the SM can lead to considerable changes in the running

of the SM parameters, including the scalar self-coupling $\lambda(Q)$. Perhaps the most dramatic manifestation of this happens in minimal models with a universal extra dimension (mUED), in which a whole set of Kaluza-Klein (KK) excitations of the SM particles appears every time we cross a threshold $Q \approx n/R$, where $n \in \mathbb{Z}$ and R is the radius of compactification [5]. In such models, the coupling constants run much faster than in most other scenarios, following a power-law behaviour [6, 7] rather than the slower logarithmic running familiar to us in the SM. This power-law running has three major consequences, viz.,

- The three gauge couplings tend to unify approximately at a scale $Q \approx 20R^{-1}$. Since it is usual to take R^{-1} somewhere around the electroweak scale, this would bring the grand unification (GUT) scale down to the order of 10 TeV, i.e. just beyond the kinematic reach of the LHC.
- If $\lambda \gtrsim 0.28$ at the electroweak scale, this self-coupling grows with energy scale Q and eventually develops a Landau pole at a scale around $45R^{-1}$. Obviously, the cutoff of this theory cannot lie beyond this scale. This leads to the well-known *triviality bound* on the mUED model.
- If $\lambda \lesssim 0.18$ at the electroweak scale, this self-coupling decreases with energy, until it is eventually driven to a negative value at an energy scale Q which is generally less than the GUT scale in this model. At this point, as explained above, the electroweak vacuum becomes unstable. This value of Q may, therefore, be referred to as the *vacuum stability bound* and we should require the theory to be cut off at this scale or lower.

The range $0.18 \lesssim \lambda(Q_{ew}) \lesssim 0.28$ is a grey area, portions of which can fall under either of the above two cases depending on exact value of the top quark Yukawa coupling at the electroweak scale, and the accuracy to which the beta functions in the theory are evaluated. However, this discussion is now a purely academic one, because we know that if the Higgs boson exists, we must have $0.12 \leq \lambda(Q_{ew}) \leq 0.13$ — which means that we are definitely faced with the scenario described in the third bullet above. One therefore, needs to ask the question, what is the vacuum stability bound, beyond which the minimal UED model must be cut off, and how many KK levels are allowed to contribute to processes generated at the loop level? This issue has already been addressed in Refs. [7, 8], for a somewhat larger range of allowed $\lambda(Q_{ew})$ than the above, each of which was consistent with the then-current bounds on the mass of the Higgs boson. We revisit the bound here, in the light of the narrow window 122 – 127 GeV in which the Higgs boson mass may be presumed to lie. We have

used the same formulae as in Ref. [7], with a top quark mass chosen to be 173.2 GeV. Our results are shown in Figure 1.

In Figure 1, we have plotted, as a function of the compactification radius R^{-1} , the ratio $\Lambda/R^{-1} = \Lambda R$. The (blue) shaded region shows the variation in this ratio as the mass of the SM Higgs boson is varied from 122 GeV to 127 GeV. Obviously, assuming tree-level masses, the number of KK modes with mass $M_n = n/R$ which can participate in any process will be given by the nearest integer less than the ordinate for a given value of R^{-1} , plotted along the abscissa. It is clear that this number will only vary between 3 and 6, and can never reach higher values such as 10 and 20 without destabilising the electroweak vacuum. Variation of the top quark mass between its experimentally allowed limits results in some minor distortion of the curves shown in Figure 1, but the conclusion remains unchanged.

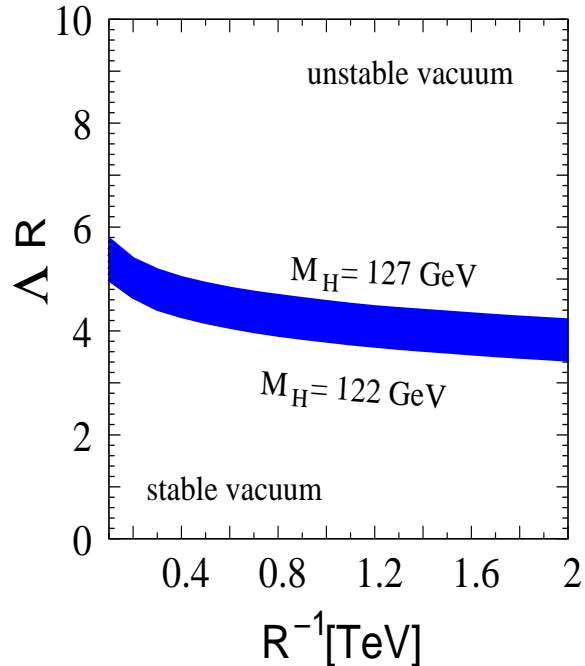


Figure 1: Variation with R^{-1} of the cutoff Λ , presented in terms of the ratio Λ/R^{-1} , as permitted by stability of the electroweak vacuum.

A similar result also follows from the constraints presented in Ref. [8]. What has not been studied in Ref. [8], however, and forms the main thrust of our work, is the serious implications such a low cutoff implies for the phenomenology of the mUED model in the context of collider searches. In the following discussions, we explore these consequences in two different contexts, viz.

1. electroweak precision tests; and
2. collider searches for mUED signatures.

Before proceeding further, we pause at this point to recall how the masses and couplings of the mUED model are generated. At the tree-level the masses M_n of all the KK excitations at the level n ($n \in \mathbb{Z}$) are given by

$$M_n^2 = M_0^2 + \frac{n^2}{R^2} \quad (1)$$

where M_0 is the mass of the SM excitation, which corresponds to the zero mode $n = 0$ of the KK tower of states. The non-observation of KK states at the LEP-2 collider, running at a centre-of-mass energy around 200 GeV, tells us that the value of R^{-1} is not less than 100 GeV. This means that for $n \geq 1$ the KK excitations all have masses in the ballpark of n/R , i.e. are almost degenerate, with a small splitting, due to the zero-mode masses M_0 . However, this is not the end of the story, for each KK mass receives quantum corrections at the loop level, i.e. we should re-write Eqn. (1) as

$$M_n^2 = M_0^2 + \frac{n^2}{R^2} + \delta M_n^2 \quad (2)$$

where the δM_n^2 represents the radiative corrections at the level of as many loops as we wish to compute. Since the couplings are usually of electroweak strength, it is usually sufficient to compute the one-loop corrections. However, it is important to note that the loop momentum will run all the way up to the cutoff scale Λ of the theory, i.e. all the KK levels n which can be included within the scale Λ would contribute to the δM_n^2 term in Eqn. (2). The detailed formulae for these corrections δM_n^2 may be found in Ref. [9], and have been used for our numerical estimates. These formulae are also implemented in a software package [10] to be run in conjunction with the Monte Carlo event generator CALCHEP [11], and we have verified that our results are in good agreement with this package.

Generally, the phenomenological results available in the literature use a cutoff $\Lambda \approx 20R^{-1}$, which is consistent with the GUT scale in a mUED scenario. Now, however, we have seen that the cutoff must be much smaller, with $\Lambda \lesssim 4R^{-1}$ instead. Thus, when only three or four KK levels contribute to the self-energy corrections in place of twenty, it is natural to assume that these radiative corrections will be significantly smaller than those predicted earlier. Since it is primarily the δM_n^2 which lift the degeneracy between different states at the same n level, one may expect the states to be rather more degenerate than had been thought earlier. This is illustrated in Figure 2, where we show the variation of the $n = 1$ masses, as a function of the ratio $M_1/R^{-1} = M_1R$, when R^{-1} varies from 100 GeV to 2.0 TeV.

The different coloured bands in Figure 2 correspond to variation of some of the important masses in the $n = 1$ KK spectrum of the mUED model, viz., the $n = 1$ excitations of the gluon (g_1), the light quarks (q_1), the W -boson (W_1), the electron (e_1) and the photon γ_1 . Of these, the γ_1 , whose mass remains more-or-less exactly at R^{-1} is clearly the LKP. The thickness of the bands in the right panel corresponds, as in Figure 1, to variation of M_H over the allowed range, with the lower (upper) edge corresponding to $M_H = 122$ (127) GeV. What strikes us immediately about the spectrum is that at the lower end, the overall splitting

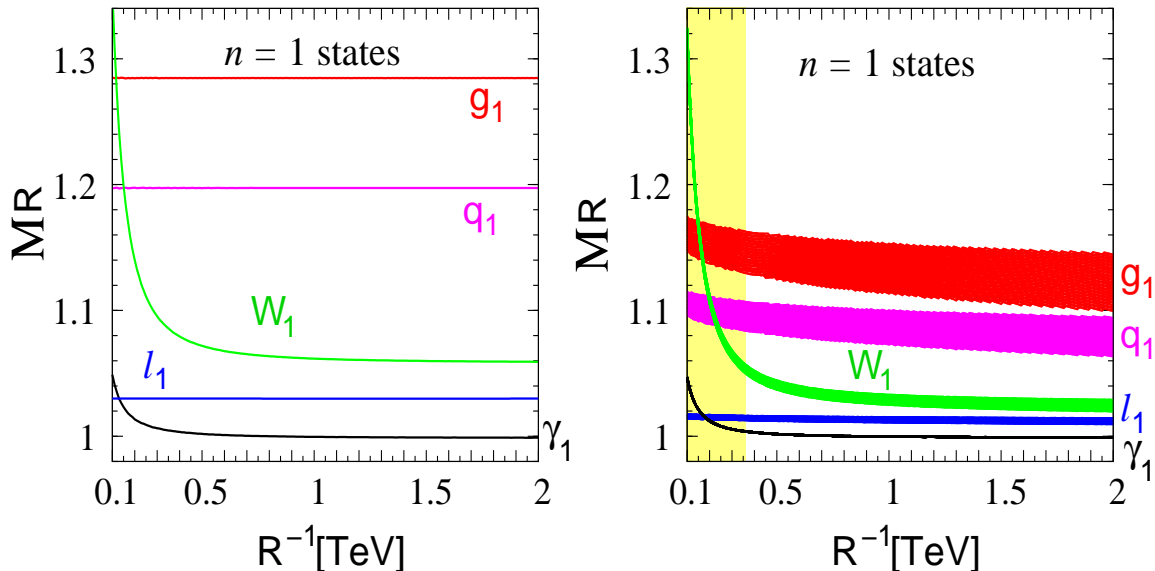


Figure 2: Variation with R^{-1} of the masses of some of the $n = 1$ KK excitations. The lines/bands coloured red, pink, green, blue and black correspond, respectively, to the masses of the g_1 , q_1 , W_1 , e_1 and γ_1 . Each mass is presented as a multiple of the common scale R^{-1} . The right panel shows the spectrum with summation over the allowed number of KK levels, while the left panel shows the spectrum with summation over 20 KK levels. The yellow-shaded region in the right panel indicates the region $R^{-1} \leq 260$ GeV, which is more-or-less ruled out by LEP data on the oblique parameters (see below).

between the lightest KK particle (LKP), viz., the γ_1 and the heaviest $n = 1$ excitation, viz., the g_1 , is never more than about 17%. By contrast, if we sum the loop corrections over 20 KK levels, we would predict a maximum splitting around 30%, i.e roughly double of what we see in Figure 2. To take a concrete example, if $R^{-1} = 500$ GeV, the mass splitting is never more than about 80 GeV, whereas if we had summed over 20 levels, we would have predicted a splitting close to 150 GeV. It is interesting that the only specific input in all of this is the newly-measured mass of the Higgs boson – the rest follows inexorably from the vacuum stability argument. Such compression of the spectrum will happen in all the KK levels, though we are most affected by the compression in the first level.

Let us now take up the consequences of this effect in the specific phenomenological contexts mentioned above. Obviously, the oldest of these constraints come from the electroweak precision tests – more specifically, from the mUED model contributions to the oblique parameters S , T and U [12]. Though these have been calculated by many authors [13], we use the simple and accurate formulae presented in Ref. [14]. Once again, we set the mass of the top quark to 173.2 GeV in our calculation. This is, in fact, an important parameter in the calculation of the oblique parameters, but we have checked that variation over the allowed

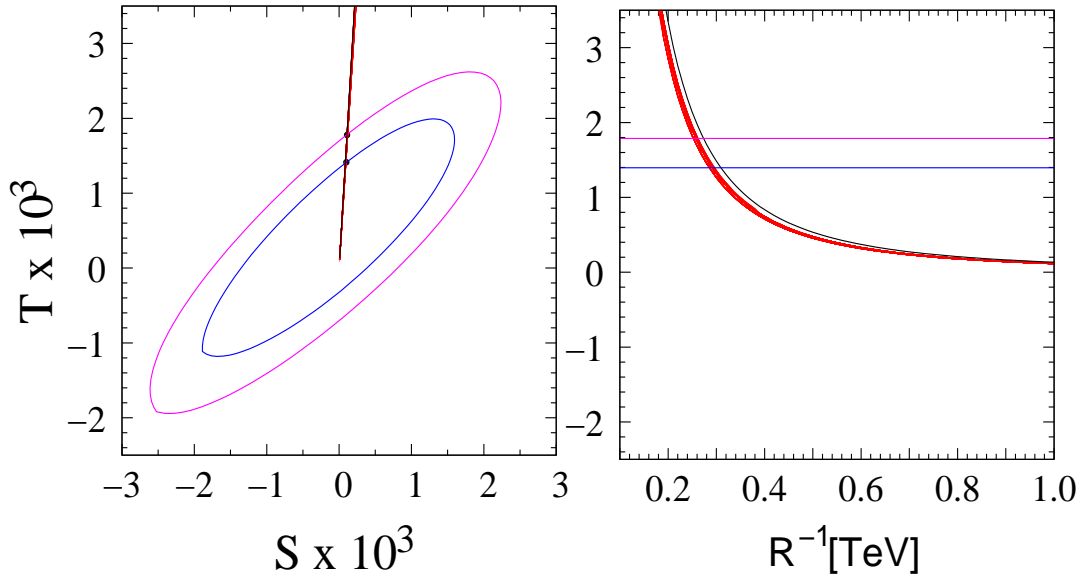


Figure 3: Oblique parameters in the $mUED$ model. Both panels show the $mUED$ contributions in red (black) depending on whether the summation over KK levels is carried out to realistic (twenty) levels. The ordinate is $T \times 10^3$ in both panels. The blue (pink) ellipses on the left panel correspond to the LEP-2 constraints at 95 (90) C.L. and the blue (pink) lines on the right panel indicate the values of ordinate for which these are crossed by the $mUED$ contributions, i.e. all values of ordinate lower than these lines are permitted by the electroweak data at 95 (90) C.L..

experimental range produces very small effects so far as the constraints on the $mUED$ model are concerned. It is, therefore, convenient to keep its value fixed and vary other important parameters, such as the Higgs boson mass M_H and the compactification radius R .

In Figure 3 we plot the deviations S and T from the SM values, so that the SM corresponds to the origin of this graph. A glance at the left panel of Figure 3 informs us that the $mUED$ contribution to the S parameter is so small that the constraint on this model arises essentially from the T -parameter, or, to use its older equivalent, the ρ -parameter. The S parameter contributes nevertheless, to the constraint through its correlation with the T -parameter, which is obvious from the fact that the allowed regions form ellipses rather than rectangles in the plots. Thus, the limits on the $mUED$ model may be read off from the plot by considering the intersection of the $mUED$ plot with the 90% and 95% C.L. ellipses. If we do this, we can demand that T will be less than 1.788 (1.396) at 90 (95)% level. Now, the black plots indicate the $mUED$ contributions when we sum over 20 levels, while the red plots indicate the same results with a realistic cutoff. The thickness of the red curves indicates the result of varying m_H over the range 122 – 127 GeV.

On the right panel of Figure 3, we have plotted the $mUED$ contribution to the T parameter

as a function of R^{-1} , with red (black) curves indicating sums over realistic (twenty) levels. The difference is rather small, and hence, the imposition of vacuum stability constraints on the mUED model results in a slight decrease in the constraint on R^{-1} . The exact results are given in Table 1 below.

levels	95%C.L.	99%C.L.
3 – 4	285 (296)	249 (261)
20	310	273

Table 1: *Lower limits (in GeV) arising from electroweak precision tests, on the compactification scale R^{-1} . The first line shows the realistic bounds, with the range corresponding to $M_H = 122(127)$ GeV respectively, while the second line corresponds to summing over 20 levels — which is unrealistic, but consistent with earlier practice.*

The numbers presented in Table 1 make it clear that the compactification scale in the mUED model must lie above the electroweak scale, viz., 246 GeV. However, the difference induced by the vacuum stability constraint are rather modest, being at a level less than 10% irrespective of the mass of the Higgs boson. On the whole, therefore, we may say that electroweak precision constraints on the mUED model essentially stand, with a slight relaxation from the earlier results.

The compression of the spectrum has much more dramatic effects when we consider collider searches for the KK excitations in the mUED model. In this context, it is first worth noting that the constraints from precision electroweak data indicate that direct searches at both the LEP-2 and Tevatron colliders would fail, as pair-production of even the $n = 1$ KK excitations is beyond the kinematic limit of these machines. It must be to the LHC, running in the range of several TeV, that we turn for these direct searches. At this point, a quick review of mUED search strategies at the LHC is needed before we can assess the impact of the compression effect on these searches.

Production modes for KK excitations at the LHC can be divided into two classes, both requiring roughly the same amount of energy, viz.,

- pair-production of $n = 1$ modes, which requires energy in the ballpark of $2 \times R^1$, since the masses of $n = 1$ modes is in the ballpark of R^{-1} ;
- resonance production of $n = 2$ modes, which requires energy in the ballpark of $1 \times 2R^1$, since the masses of the $n = 2$ modes is in the ballpark of $2R^{-1}$.

mUED searches based on the first of these, namely pair-production of $n = 1$ states, are very reminiscent of searches for supersymmetry, resulting in the appellation 'bosonic supersymmetry' for the mUED model. The principal modes for such pair production involve the strongly-interacting $n = 1$ states and are

$$pp \rightarrow \begin{cases} g_1 + g_1 \\ q_1 + \bar{q}_1 \\ g_1 + q_1(\bar{q}_1) \end{cases} \quad (3)$$

where q stands for any quark flavour, either singlet or doublet, with the top quark included if it is kinematically possible. The g_1 will always decay as

$$g_1 \rightarrow \begin{cases} q + \bar{q}_1 \\ q_1 + \bar{q} \end{cases} \quad (4)$$

with a hadronic jet arising from the q or \bar{q} , as the case may be. Obviously, since the gluon coupling is vectorlike, equal numbers of doublet q_{1L} and singlet q_{1R} states will be produced. Decays of these q_1 states involve more channels, viz.,

$$q_{1L} \rightarrow \begin{cases} q + \gamma_1 \\ q + Z_1^0 \rightarrow q + \ell^\pm + \ell_1^\mp \rightarrow q + \ell^+ \ell^- + \gamma_1 \\ q' + W_1^\pm \\ \quad \hookrightarrow W^\pm + \gamma_1 \quad \rightarrow \ell^\pm + \nu(\bar{\nu}) + \gamma_1 \\ \quad \quad \quad \hookrightarrow q\bar{q} + \gamma_1 \\ \quad \hookrightarrow \nu(\bar{\nu}) + \ell_1^\pm \quad \rightarrow \nu(\bar{\nu}) + \ell^\pm + \gamma_1 \\ \quad \hookrightarrow \ell^\pm + \nu_1(\bar{\nu}_1) \quad \rightarrow \nu(\bar{\nu}) + \ell^\pm + \gamma_1 \end{cases} \quad (5)$$

and

$$q_{1R} \rightarrow \begin{cases} q + \gamma_1 \\ q + Z_1^0 \rightarrow q + \ell^\pm + \ell_1^\mp \rightarrow q + \ell^+ \ell^- + \gamma_1 \end{cases} \quad (6)$$

with the final states in Eqn. 5 being, from top to bottom, hadronic jet plus missing E_T (MET), hadronic jet plus dilepton plus MET, single lepton plus MET, pair of jets plus MET, single slepton plus MET, single lepton plus MET; while the final states in Eqn. 6 are, from top to bottom, hadronic jet plus missing E_T (MET) and hadronic jet plus dilepton plus MET. Here we must remember that the number of jets is only a rough estimate, since jets can always split and/or merge during the fragmentation process.

When we consider all the possible cascade decays of the pair of q_1, g_1 states produced, it is obvious that the final states will always involve (a) large missing transverse energy (MET),

and (b) an indeterminate but limited number of hard leptons and jets — where the word ‘hard’ is used not so much in the usual sense of large transverse momentum (p_T) but more to distinguish these from ‘soft’ leptons and jets produced during fragmentation. The reason for this last caveat is that the transverse momentum carried by these arises almost wholly from the mass difference between the parent and daughter states, which, in a compressed mUED mass spectrum, is not very large. The question then arises as to whether these leptons and hadronic jets can clear the minimum p_T cuts employed in mUED searches. To study, this, it is clear that the relevant mass differences, with the corresponding states, are

1. jet: $M(g_1) - M(q_1)$, or, $M(q_1) - M(\gamma_1)$, or, $M(q_1) - M(W_1)/M(Z_1)$;
2. lepton: $\frac{1}{2} [M(Z_1) - M(\ell_1)]$, or, $\frac{1}{2} [M(W_1) - M(\gamma_1)]$, or, $M(\ell_1) - M(\gamma_1)$.

We must note that these mass differences form approximate upper bounds on the transverse momentum p_T ; for most events the actual p_T value is lower. We also note in passing that though we will present mass differences for the choice $q_1 = u_{1L}$, there will be very little change if any of the others is chosen.

One of the most important results of having a compressed spectrum is that for a given value of R^{-1} , the masses of the q_1 and g_1 states are lighter than before, and hence, these would be produced more copiously at the LHC. To illustrate this, as well as the upper bounds on jet and lepton p_T , we have plotted, in Figure 4, the total production cross-sections at the 14(7) TeV LHC for the processes listed in Eqn. 3 versus the mass differences

- (a) $M(g_1) - M(q_1)$;
- (b) $M(q_1) - M(\gamma_1)$;
- (c) $\frac{1}{2} [M(W_1) - M(\gamma_1)]$;
- (d) $M(\ell_1) - M(\gamma_1)$.

In every plot, the solid (broken) lines indicate a Higgs boson mass of 127 (122) GeV, while the colour red(blue) corresponds to 14 (7) TeV. The value of R^{-1} varies from 300 GeV to several TeV as we proceed downwards along each line. Cross-sections obviously tend to decrease as the Higgs boson mass increases, and this is accentuated at larger values of R^{-1} .

A striking feature of the plots shown in Figure 4 is the fact that the raw cross-sections for production of $n = 1$ particles can be very large – several nanobarns for low values of R^{-1} , but fall rapidly as R^{-1} increases. This is not surprising, for after all, it is known that the $t\bar{t}$ production cross-section is close to a nanobarn, and the heavy q_1 states are, after all, very similar to top quarks. For the same reason, however, $t\bar{t}$ production could be an irreducible

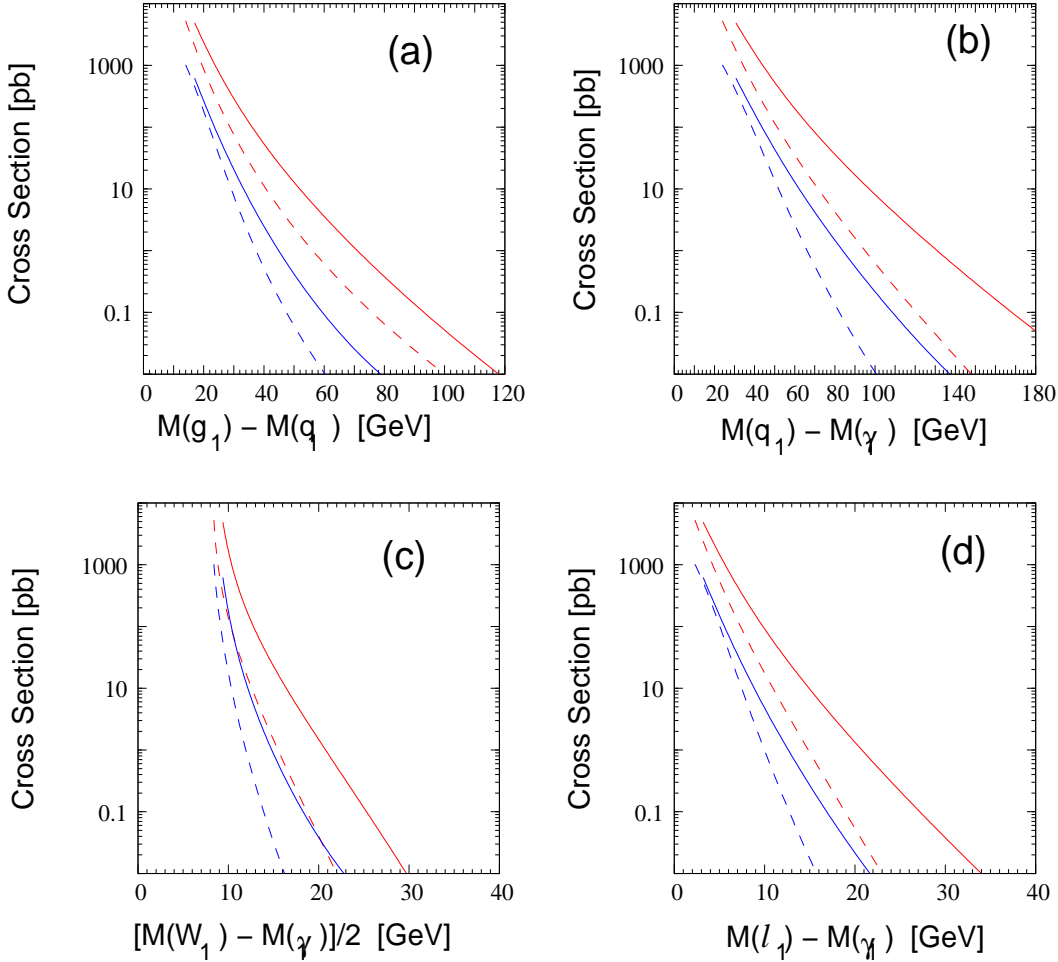


Figure 4: Cross-sections for g_1 and q_1 pair production (see Eqn. (3)) at the LHC, versus various mass differences as labelled corresponding to the maximum energies of (a,b) jets, (c) jets and leptons, and (d) leptons, arising in the cascade decays of $n = 1$ KK resonances. Solid (broken) lines correspond to $M_H = 127$ (122) GeV, while the colours red(blue) correspond to $\sqrt{s} = 14$ (7) TeV respectively.

background to mUED signals, since the top quark and its anti-quark are known to decay to leptons, hadronic jets and large MET. In, fact, to get rid of the $t\bar{t}$ and other SM backgrounds, including the enormous QCD background, it is usual to impose some minimum cuts on the p_T of these final states. This, we shall see, will deeply affect the kind of searches we are now considering. For, as the plots in Figure 4 show, the p_T of the final states leptons and jets is severely limited by the small mass differences in the compressed spectrum. As a result, p_T cuts imposed to remove SM backgrounds will also remove substantial portions of the mUED signals. In fact, the low cross-sections for $\sqrt{s} = 7$ TeV, illustrated in Figure 4, lead us to believe that we must look to the 14 TeV option to see any viable signal.

Let us consider the mUED signals in some more detail. If we go by the analogy of supersym-

metry, the most promising final state should be multiple jets and large missing transverse energy (MET). Typical p_T triggers for multi-jet plus MET signals in supersymmetric models generally lie at the level of 50 to 100 GeV, and it is clear from Figure 4 (a) and (b) that the mUED signal events would be able to clear such trigger requirements only for larger values of R^{-1} , where the cross-sections are rather small. However, if the trigger requirements are relaxed in a low- p_T search, the situation does not improve substantially, for then the SM backgrounds become intractable. To make matters concrete, we carry out a Monte Carlo simulation of the signal with multiple jets and MET at $\sqrt{s} = 14$ TeV, using the well-known Monte Carlo event generator PYTHIA [15], for $R^{-1} = 500$ GeV, with weak and strong kinematic criteria as follows:

C0: only lepton veto;

C1: lepton veto, $p_T^J \geq 20$ GeV and $\cancel{E}_T \geq 30$ GeV;

C2: lepton veto, $p_T^J \geq 50$ GeV, $\cancel{E}_T \geq 100$ GeV.

The 'lepton veto' requires the absence of isolated leptons with transverse momentum greater than 10 GeV. Our results are given in Table 2 below.

cuts	model	≤ 2 jets + \cancel{E}_T	3 jets + \cancel{E}_T	4 jets + \cancel{E}_T	> 4 jets + \cancel{E}_T
C0	mUED	116.9 (97.4)	66.6 (63.4)	44.2 (41.5)	37.9 (43.8)
C1	mUED	86.4 (74.8)	55.0 (53.3)	39.1 (36.9)	35.6 (40.8)
	SM ($t\bar{t}$)	2.9	7.4	12.3	23.3
	SM (QCD)	1432.4	1386.3	850.1	612.5
C2	mUED	4.56 (3.12)	1.08 (1.4)	0.58 (0.67)	0.16 (0.31)

Table 2: The mUED signal in pb corresponding to $R^{-1} = 500$ GeV and $M_H = 122$ (127) GeV and SM backgrounds in the multi-jets + MET channels at the 14 TeV LHC, showing the effect of selection criteria defined by (C0) only lepton veto; (C1) lepton veto, $p_T^J \geq 20$ GeV, $\cancel{E}_T \geq 30$ GeV; (C2) lepton veto, $p_T^J \geq 50$ GeV, $\cancel{E}_T \geq 100$ GeV. All detection efficiencies are assumed to be unity.

It is clear from Table 2 that, irrespective of the exact mass of the Higgs boson, the mUED signal is at the level of a couple of hundred picobarns. This may appear sizeable, but it is not really so when we consider the SM backgrounds, of which we have presented just two, viz. $t\bar{t}$ production, and QCD production of jets and MET. Merely taking these two signals adds up to a few *nanobarns*, against which there is no hope of discerning the mUED signals. We can, of course, reduce the SM background by imposing more stringent kinematic cuts on the jets as well as on the MET. However, these will prove more deadly for the tenuous signal than for the background. For example, imposing $p_T^J \geq 50$ GeV and requiring MET greater than 100 GeV effectively reduces the signal by one, or even two, orders of magnitude,

thereby offsetting any advantage to be gained by imposing stricter kinematic criteria on the background. One may safely conclude, therefore, that even though $n = 1$ KK states will be copiously produced at the LHC, it will be very difficult to isolate them from the background, in the multi-jets plus MET channel.

Recently, a combination of event shape variables has been used rather effectively [17] to reduce the SM backgrounds to the signal with multiple jets and MET. This has proved very successful for searches for supersymmetry, where the final state jets are hard and there is considerable MET. An allied study [18] of mUED signals using the same technique claims that this can be effectively used to search for mUED in the jets plus MET channel. However, we note that the success of this technique depends rather crucially on the ‘hardness’ of the jets, and Ref. [18] achieves this by taking $\Lambda R = 10$ and 40. We suspect that if the same analyses were to be re-done using the correct values of ΛR as presented in this article, the result would prove as disappointing as that for conventional searches described above.

We now turn to leptonic signals for mUED. Naively, a glance at Figure 4 would make matters seem very gloomy for such signals, since the p_T of the leptons, whose upper bounds correspond to the abscissa in Figure 4 (c) and (d), rises above the trigger level of 20 GeV only when the cross-section falls to very low values. However, if the trigger level is reduced to, say, 10 GeV, the mUED signal will be less affected, but will now have to compete with SM backgrounds involving soft leptons arising from electroweak sources as well as hadronic decays inside jets. It is difficult to guess what will happen without performing a detailed study, and hence, we have again performed a simulation of the multi-lepton signals at $\sqrt{s} = 14$ TeV, using PYTHIA, for $R^{-1} = 500$ GeV, and imposing various kinematic criteria:

$$\text{C1: } p_T^\ell \geq 10 \text{ GeV, } \cancel{E}_T \geq 20 \text{ GeV;}$$

$$\text{C2: } p_T^\ell \geq 20 \text{ GeV, } \cancel{E}_T \geq 30 \text{ GeV;}$$

$$\text{C3: } p_T^\ell \geq 20 \text{ GeV, } \cancel{E}_T \geq 50 \text{ GeV;}$$

$$\text{C4: } 10 \text{ GeV} \leq p_T^\ell < 25 \text{ GeV, } 10 \text{ GeV} \leq \cancel{E}_T < 25 \text{ GeV.}$$

Our results are illustrated in Table 3.

A close study of Table 3 reveals the following features. Focussing on the mUED signal, it is clear that one may expect reasonably large cross-sections for signals with leptons, jets and MET, with lepton multiplicities of 1, 2 and 3, but a somewhat diminished probability of producing 4 leptons. This is easy to motivate from the decay chains listed in Eqns. 5 and 6. However, the application of even so gentle a kinematic selection criterion as C1: $p_T^\ell \geq 10$ GeV,

$\cancel{E}_T \geq 20$ GeV leads to a considerable diminution of the signal in all channels except the one with a single lepton where the numbers are obviously not competitive with the SM backgrounds shown immediately below, which arise mainly from the production and decay of W, Z states, with or without associated jets, from $t\bar{t}$ production, and from QCD jets, which generate a hard isolated lepton only once in a few millions, but nevertheless form a substantial background because of the enormous cross-section for QCD processes. The QCD background is negligible for the case of two or more leptons, but there is a large background to dileptons from electroweak processes including the $t\bar{t}$ decays.

cuts	model	$1l + \text{jets} + \cancel{E}_T$	$2l + \text{jets} + \cancel{E}_T$	$3l + \text{jets} + \cancel{E}_T$	$4l + \text{jets} + \cancel{E}_T$
		σ (pb)	σ (pb)	σ (fb)	σ (fb)
C1	mUED	76.6 (81.8)	10.39 (11.9)	725.3 (1 002.0)	54.0 (67.2)
	SM (EW, $t\bar{t}$)	62 758.0	5 041.9	90.8	3.5
	SM (QCD)	30 420.0	0.0091	–	–
C2	mUED	11.56 (14.3)	0.43 (0.7)	14.1 (7.0)	1.1 (0.9)
	SM (EW, $t\bar{t}$)	52 612.7	3 884.2	77.2	2.3
C3	mUED	9.47 (11. 2)	0.31 (0.5)	14.0 (3.5)	7.1 (0.4)
	SM (EW, $t\bar{t}$)	52 612.7	3 884.2	77.2	2.3
C4	mUED	10.35 (9.5)	1.27 (1.4)	54.5 (91.4)	2.0 (11.3)
	SM (EW, $t\bar{t}$)	16 434.1	892.1	0.5	0.1

Table 3: The mUED signal corresponding to $R^{-1} = 500$ GeV and $M_H = 122$ (127) GeV and SM backgrounds in the multi-lepton + jets + MET channels at the 14 TeV LHC, showing the effect of selection criteria defined by (C1) $p_T^\ell \geq 10$ GeV, $\cancel{E}_T \geq 20$ GeV; (C2) $p_T^\ell \geq 20$ GeV, $\cancel{E}_T \geq 30$ GeV; (C3) $p_T^\ell \geq 20$ GeV, $\cancel{E}_T \geq 50$ GeV; (C4) 10 GeV $\leq p_T^\ell < 25$ GeV, 10 GeV $\leq \cancel{E}_T < 25$ GeV. All detection efficiencies are assumed to be unity.

Very different from the case of one or two leptons are the two columns on the right of Table 3. Here, the trilepton and quadrilepton signals stand out clearly over the backgrounds, when the milder selection criteria C1 and C4 are taken (the converse is the case when we take more conventional criteria as in C3 and C4). For the trilepton signal, the signal will be substantial even in the early runs of the 14 TeV LHC upgrade; for the quadrilepton signal, the signal is more modest, and will require perhaps a year or two to show up in enough numbers to come to any definite conclusion. .

Searches for the mUED model at the LHC will, therefore, clearly have to wait a few years before any conclusion can be reached. Noting that all our results are pertinent to a comparatively low $R^{-1} = 500$ GeV, a negative result will only push up the lower bound on R^{-1} to

a higher value, perhaps eventually in the ballpark of 1.5 TeV. On the other hand a positive signal will hardly be distinguishable from those of a supersymmetric model with a similarly compressed spectrum. It may be mentioned in passing that it has been claimed [19] that the multiplicity of accompanying jets can be used as a discriminant between the mUED and supersymmetric models. Such claims are, however, based on studies with a less compressed spectrum and much more stringent kinematic cuts on the leptons, accompanying jets, and MET. Their applicability to a compressed mass spectrum as considered in this work is, therefore, an open question.

Another way to easily distinguish mUED signals from supersymmetric ones involves looking for the $n = 2$ KK excitations. Here, however, the situation is really gloomy. Once again, the spectrum will be compressed – at the same relative level as that for $n = 1$ states, though the splitting would be roughly double that for $n = 1$ states. Referring to Figure 2, we see that for $R^{-1} = 1$ TeV, we can expect a γ_2 of mass around 2.0 TeV, a W_2 and a Z_2 of mass around 2.08 TeV and a g_2 of mass around 2.22 – 2.26 GeV. These states can be produced singly as resonances in quark or gluon fusion, and can be detected through their subsequent decay into $\ell^+\ell^-$ pairs [16] or $t\bar{t}$ pairs [20].

Compression of the mass-spectrum does not really matter for the single production of resonances, but in such studies, what really matters is the coupling of the resonance to the partons, which is achieved through KK number-violating operators generated at the one-loop level. Obviously, such couplings, like the mass-splitting, will be seriously affected by the number of KK levels over which the loop momentum is summed. An estimate of this effect may be obtained from Figure 2 of Ref. [20], where the sum over 5 KK levels may be taken to closely approximate the effect of the sum over 3–4 levels induced by the vacuum stability condition. At a rough estimate, the result of the lower number of KK levels summed leads to a reduction of the couplings of the g_1 to partons by a factor around 4 to 5, i.e. a reduction in the resonant cross-section by a factor around 20. If we apply this to the results shown (for $\Lambda R = 20$) in Figure 6 of Ref. [20], the nice resonances shown therein shrink to levels which are smaller even than the 1σ fluctuation in the $t\bar{t}$ background from the SM. As the relevant plot already assumes a luminosity of 100 fb^{-1} at 14 TeV, it is more-or-less obvious that g_2 resonances, like the $n = 1$ cascade products, will be lost against the SM backgrounds. A similar argument may be applied to γ_2 and Z_2 resonances, decaying to e^+e^- and $\mu^+\mu^-$ pairs, illustrated in Figure 9 of Ref. [16]. In this case, the reduction in the coupling is by a factor around 10 rather than 20, but this will still leave barely one or two

signal events to be discovered in 100 fb^{-1} of data, against a background in the ballpark of $10 - 20$ events. Thus, the search for $n = 2$ states seems to be another issue without hope.

It is quite clear, therefore, that if a Higgs boson is discovered in the now-relevant mass range of $122 - 127 \text{ GeV}$, this will immediately render sterile all prospects of finding mUED signals at the LHC, except in the trilepton and quadrilepton channels — where they will be indistinguishable from a class of models with supersymmetry. One can, then ask the legitimate question whether it is better worth looking for such signals at the proposed International Linear Collider (ILC), where e^+e^- pairs will collide at energies of 500 GeV or 1 TeV . Indeed e^+e^- colliders are known to be much cleaner as regards SM backgrounds, and this might make it easier to find the elusive mUED signals and try to distinguish them from supersymmetry signals [21]. Of course, the bounds on R^{-1} arising from electroweak precision tests tell us that we cannot expect to produce KK excitations in the 500 GeV run. At the 1 TeV run, searches for $n = 2$ resonances excited by ‘return to the Z' -type effects due to ISR and beamstrahlung could result in narrow resonances in dilepton channels [21], but these cannot survive the order-of-magnitude reduction in coupling described above. For $n = 1$ states, a detailed study made in the context of the 4 TeV CLIC machine [22] shows that to detect signals with leptons and missing energy, one requires a minimum of 50 GeV of MET, which cannot be achieved through $n = 1$ KK mode decays involving leptons. Prospects may be better for the signal arising from

$$e^+e^- \rightarrow q_1 + \bar{q}_1 \rightarrow (q + \gamma_1) + (\bar{q} + \gamma_1) \quad (7)$$

which involves two jets and MET. Here the SM backgrounds may be more tractable than in a hadron collider like the LHC, but a more focussed study is required to confirm this guess [23].

In conclusion, then, we have shown that if a light Higgs boson is indeed found at the LHC, the collider phenomenology of a mUED model would be profoundly affected by the low cutoff demanded by the vacuum stability of the model. At the LHC, the $n = 1$ states will be produced in large numbers, but will decay into soft final states indistinguishable from the QCD and other SM backgrounds, except for weak trilepton and quadrilepton signals with accompanying jets and MET. The $n = 2$ particles could appear as resonances in dilepton and $t\bar{t}$ final states, but these may be too weak to appear above the SM backgrounds. For $n = 2$ states, a similar conclusion will hold at the ILC or CLIC machines, but the dijet plus MET signal has better prospects. If, indeed, the mUED picture of the world is correct, we may have to wait for the upgraded LHC to make the discovery and for the ILC to be up and

running at 1 TeV before we can come to a definite conclusion.

Acknowledgements: The authors would like to thank the organisers of the WHEPP-XII (Mahabaleshwar, India), where this problem was conceived and discussed. AD, whose work is partially supported by the UGC-DRS programme acknowledges computational help from Kirtiman Ghosh. Thanks are also due to Dipan Sengupta (CMS Collaboration) for supplying some of the numbers presented in Table 2, to Avirup Shaw for helping to make some of the graphs, and to Shruti Singh for computer support.

References

- [1] G. Aad et al (ATLAS Collaboration), Phys. Lett. **B716**, 1 (2012);
S. Chatrchyan et al (CMS Collaboration), Phys. Lett. **B716**, 30 (2012);
TEVNPH Working Group (for the CDF, D0 Collaborations), Fermilab preprint FERMILAB-CONF-12-318-E, arXiv:1207.0449 [hep-ex] (2012).
- [2] ATLAS Collaboration, ATLAS NOTE ATLAS-CONF-2012-162 and CMS Collaboration, CMS Note CMS PAS HIG-12-045 (results presented at the HCP Conference, Kyoto, 2012).
- [3] J. Elias-Miro *et al*, Phys. Lett. **B709**, 222 (2012);
G. Degrandi, *et al*, JHEP **1208**, 098 (2012);
F. Bezrukov, M.Y. Kalmykov, B.A. Kniehl and M. Shaposhnikov, JHEP **1210**, 140 (2012);
M. Holthausen, K.S. Lim and M. Lindner, JHEP **1202**, 037 (2012).
- [4] S. Alekhin, A. Djouadi and S. Moch, Phys. Lett. **B716** 214 (2012).
- [5] T. Appelquist, H.C. Cheng, B.A. Dobrescu, Phys. Rev. **D64**, 035002 (2001).
- [6] K.R. Dienes, E. Dudas, T. Gherghetta, Phys. Lett. **B436**, 55 (1998);
Nucl. Phys. **B537**, 47 (1999).
- [7] G. Bhattacharyya *et al*, Nucl.Phys. **B760**, 117 (2007).
- [8] M. Blennow *et al*, Phys. Lett. **B712**, 419 (2012).
- [9] H.-C. Cheng, K.T. Matchev, M. Schmaltz, Phys. Rev. **D66**, 036005 (2002).
- [10] A.K. Datta, K.C. Kong, K.T. Matchev, New J. Phys. **12**, 075017 (2010).

- [11] A. Pukhov, arXiv:hep-ph/0412191.
- [12] M.E. Peskin, T. Takeuchi, Phys. Rev. Lett. **65**, 964 (1990);
Phys. Rev. **D46**, 381 (1992).
- [13] T. Appelquist, H.U. Yee, Phys. Rev. **D67**, 055002 (2003);
T. Fläcke, D. Hooper, J. March-Russell, Phys. Rev. **D73**, 095002 (2006).
- [14] I. Gogoladze, C. Macesanu, Phys. Rev. **D74**, 093012 (2006).
- [15] T. Sjöstrand, S. Mrenna, P.Z. Skands, JHEP **0605**, 026 (2006).
- [16] A.K. Datta, K.C. Kong, K.T. Matchev, Phys. Rev. **D72**, 096006 (2005);
Erratum-ibid. **D72**, 119901 (2005).
- [17] L. Randall, D. Tucker-Smith, Phys. Rev. Lett. **101**, 221803 (2008);
A. Banfi, G.P. Salam, G. Zanderighi, JHEP **1006**, 038 (2010);
M. Guchait, D. Sengupta, Phys. Rev. **D84**, 055010 (2011).
- [18] A. Datta, A. Datta, S. Poddar, Phys. Lett. **B712**, 219 (2012).
- [19] B. Bhattacharjee *et al*, Phys. Rev. **D81**, 035021 (2010).
- [20] B. Bhattacharjee *et al*, Phys. Rev. **D82**, 055006 (2010).
- [21] B. Bhattacharjee *et al*, Phys. Rev. **D78**, 115005 (2008).
- [22] M. Battaglia *et al*, JHEP **0507**, 033 (2005).
- [23] A. Datta, S. Raychaudhuri, *work in progress*.